Open access • Proceedings Article • DOI:10.2514/6.1975-757

Analytical displacements and vibrations of cantilevered unsymmetric fiber composite laminates — Source link

M. D. Minich, C. C. Chamis

Institutions: Glenn Research Center

Published on: 01 Jan 1975

Topics: Composite laminates, Finite element method, Stiffness matrix and Cantilever

NASA TECHNICAL MEMORANDUM

NASA TM X-71699

NASA TM X-71699

ANALYTICAL DISPLACEMENTS AND VIBRATIONS OF CANTILEVERED UNSYMMETRIC FIBER COMPOSITE LAMINATES

by M. D. Minich and C. C. Chamis
Lewis Research Center
Cleveland, Ohio 44135

TECHNICAL PAPER to be presented at
Sixteenth Structures, Structural Dynamics
and Materials Conference sponsored by
the American Institute of Aeronautics and
Astronautics, American Society of Mechanical
Engineers, and Society of Automative Engineers
Denver, Colorado, May 27-29, 1975

ANALYTICAL DISPLACEMENTS AND VIBRATIONS OF CANTILEVERED UNSYMMETRIC FIBER COMPOSITE LAMINATES

M. D. Minich and C. C. Chamis
National Aeronautics and Space Administration
Lewis Research Center
Cleveland, Ohio

E-8306

Abstract

A fiber composite flat cantilever plate that has symmetric and nonsymmetric laminate configurations is theoretically investigated to determine its static and dynamic structural response. The finite element analysis method used includes a unique triangular finite element developed at Lewis for the analysis of fiber composite airfoils. The various responses investigated include tip displacements, natural frequencies, and fundamental mode shapes. The results show that laminate configurations may be selected for a cantilever such that when the tip at the leading edge is loaded normal to the plane of the plate, the tip at the trailing edge can (a) deflect in the opposite direction, (b) deflect about the same, or (c) deflect more than the tip at the leading edge. This variation in response can be utilized to provide built-in structural damping to resist flutter. The results also show that the displacements and the natural frequencies can be in considerable error for nonsymmetric laminate configurations if the membrane-bending coupling is not taken into account. Structural response results obtained from ten laminate configurations are presented in tabular forms and may be used as an aid in selecting laminate configurations for composite airfoils.

Introduction

Fiber/resin composite laminates are being used or proposed for use in structural components such as wings, horizontal and vertical stabilizers for airplanes, helicopter and wind-energy machine blades, and fan blades for aircraft turbine engines. Laminates for these types of components have a large number of plies oriented at different directions and are selected to meet design requirements for strength and stiffness.

Current practice is to design the aforementioned components using laminate configurations which are balanced (no in-plane shear-stretch-coupling) and are symmetric (with respect to bending). One reason symmetric laminate configurations have been studied extensively for these components is that they are amenable to solution using well-known analysis methods.[1,2] On the other hand, unbalanced and/or nonsymmetric laminate configurations may possess shear-stretch, bend-stretch, and/or bend-twist coupling responses (Appen. 1 of Ref. 3). Laminates with these coupling responses are difficult to analyze[4] and partly for this reason, have been avoided for use in structural components.

Some important reasons for investigating laminates having coupling responses are:

1. It may be possible to select coupling in laminates that will provide built-in self-damping mechanisms when subjected to dynamic excitations.

2. Structural components fabricated from fiber composite laminates are occasionally found to be warped and it is believed that the warpage is largely due to coupling responses that result from fabrication errors in orienting the various plies.[5]

To date, loading displacements of cantilevered laminates with coupling responses have not been investigated theoretically. In addition, the vibration responses of these laminates have received only limited theoretical investigation using primarily indirect methods.[4]

The main objective of this investigation was to investigate the displacements and vibrations of cantilevered flat laminates with various types of coupling responses. Two secondary objectives were:

1. To identify some coupling responses which may give rise to built-in self-damping mechanisms.

2. To indicate how molds may be contoured to permit, or restrain, warpage resulting from fabricating laminates that have various coupling responses.

An analysis method was used which utilizes a finite element developed at Lewis for the analysis of aircraft gas turbine fiber composite fan blades. A summary of the equations defining the element stiffness matrix is given in the appendix.

The cantilever used in the investigation is a rectangular plate with aspect ratio (a/b) equal to 2 (Fig. 1). For the displacement response, the cantilever was loaded with a concentrated load normal to the plane of the plate at the leading edge tip. For the vibration response, the cantilever was free of loads. Fiber composite laminates with various coupling responses were selected to illustrate the effects of these coupling responses on the displacements and vibration frequencies of a cantilevered plate.

The effects of the coupling responses were also investigated using the reduced stiffness (reduced bending rigidities) concept (Ref. 3, Appendix 1).

Laminate Geometry and Configuration

The structural component chosen for this investigation was a cantilever plate represented schematically in Figure 1. The reason for selecting this component is that it conveniently simulates an airfoil. The aspect ratio (length/width) equals two and the width-to-thickness ratio equals ten. The dimensions of the cantilever are $a = 2$ inches, $b = 1$ inch, and $h = 0.1$ inch (Fig. 1).

Ten different laminate configurations were selected for investigation. The ply orientations for these laminate configurations are shown schematically in Figure 2; twelve plies of equal thickness were chosen for these laminates. Four cases are symmetric with respect to bending (cases I to III,

and V); the other six cases are nonsymmetric. Note that case I has all 12 plies at 0° and case V has 6 plies at 0°, and 6 plies at 90°. These are the only cases with orthotropic material behavior.

The composite material chosen was Thornel-75-S/epoxy with a fiber volume ratio of 0.6. The plate constitutive properties (force-deformation relationships A_{ij}, C_{ij}, and D_{ij}) were computed using the program described in Reference 6 and are tabulated in Table 1. (Also see the Appendix.) The A_{ij}, C_{ij}, and D_{ij} matrices are symmetric, thus, only the upper triangular portion is given. Note that for the symmetric laminates (symmetric with respect to bending) the C_{ij}'s are zero, characteristic of the fact that no bend-stretch coupling exists for these cases. Note also that all cases except cases I and V in Table 1 have either some nonzero C_{ij} terms, A_{13}, A_{23} terms, or D_{13}, D_{23} nonzero terms. These cases exhibit anisotropic material behavior. In the reduced stiffness concept the A_{ij} and C_{ij} arrays are incorporated into D_{ij} via the following: $D^{R}_{ij} = D_{ij} - C^{T}_{ij}A^{-1}_{ij}C_{ij}$ where D^{R}_{ij} is the laminate reduced bending stiffness. The reduced bending stiffness coefficients for D^{R}_{ij} are given in Table 2 for the laminates investigated.

Method of Analysis

The analysis uses a unique triangular thin-plate finite element. This element is deduced from a thin-shell, double-curvature, variable-thickness, isoparametric, anisotropic finite element which was generated for the analysis of composite airfoils (Fig. 3). The element has six nodes (3-corner, 3-midside), each with five displacement degrees of freedom (DOF), consisting of three translation displacements, u, v, and w, and two rotations, α and β. The displacements within the element are represented by parabolic interpolation functions. The coordinate system within the element uses the same interpolation formula as the displacement; therefore the element is isoparametric (see Appendix). The strain-displacement equations used in the formulation are from thin-shell theory and include double-curvature, bend-stretch coupling, and through-the-thickness shear. The assumption that plane sections remain plane after bending is relaxed. The equations for the element stiffness matrix are summarized in the Appendix.

The thickness of the element is an input parameter at each node. The material coupling responses are represented by the twenty four coefficients which are required to describe the force-deformation relationships within the element. These coefficients are elements in the A_{ij}, C_{ij}, and D_{ij} matrices mentioned previously and tabulated in Table 1 for the cases investigated. The element stiffness and master (global) stiffness matrices are assembled in the conventional way to yield the global system of equations $F = Ku$, where F represents the nodal forces, K the master stiffness matrix, and u the nodal displacements. The solution of the system $F = Ku$ is obtained by solving this system for the displacement variables (u).

The consistent mass matrix (M) is generated using the previously mentioned parabolic interpolation functions. In addition the mass density of the element can be a variable and is therefore given as input at the individual nodes. The matrix equation, $Ku + M\frac{d^2}{dt^2}(u) = 0$, is solved for the eigenvalues and eigenvectors using available eigenvalue extraction routines. This allows the calculation of the natural frequencies and the normalized mode shapes for structures that the finite element has been intended to represent. The element formulation was checked against known solutions for both displacements and natural frequencies.

Results and Discussion

The results discussed herein include nodal displacements due to a concentrated load normal to the plane of the plate at the leading edge tip, using both 5 and 3 DOF models with 4 and 16 elements (Fig. 4) and also the first six fundamental frequencies (harmonics) with their corresponding mode shapes (Fig. 5). Results from laminates with coupling are compared to corresponding results obtained using the reduced stiffness concept.

Catilever Tip Deflections

Table 3(a) gives in tabular form the tip deflection from the leading edge (LE) to the trailing edge (TE) at the quarter stations (Fig. 4(b)) for the cantilever (Fig. 1) without bend-stretch coupling (only bending variables). This model consisted of 16 elements (Fig. 4(b)) with three displacement DOF (w, α, β) per node resulting in 120 free variables. The applied load for all the displacement results was a 15-pound concentrated load at the tip at the leading edge. The aluminum case is included to illustrate the corresponding behavior of a typical isotropic material. Table 3(b) gives the displacement results with five displacement DOF per node (200 variables total). The effect of bend-stretch coupling (nonsymmetry) is evident when the displacements for cases IV, VI to X given in Table 3(b) are compared with the corresponding results given in Table 3(a). It was previously pointed out that case I is the orthotropic case where all 12 plies are in the longitudinal direction. This is the stiffest case and exhibits a slight downward displacement at the trailing edge. Case X has very slight material bend-stretch coupling but it is noted that the trailing edge has a displacement larger than that obtained at the leading edge where the load is applied. With the ply orientation of cases IV and X, deflections are obtained which are very large compared to the orthotropic case. Table 3(c) gives the displacement results for the material coupling cases using the reduced stiffness values in Table 2. Only the bending variables are used with the reduced stiffness. Thus, the total number of variables decreases from 200 to 120. As can be seen the results obtained are comparable to those given in Table 3(b).

The previous discussion leads to the following important observation. Since the deformed shape for unsymmetric laminates is calculable, laminate configurations may be selected with predetermined twist (untwist) for anticipated membrane and bending loads. This can be used to offset increasing angle of attack in airfoil designs and thereby provide structural damping to minimize or avoid flutter. Also the predetermined deformation can be used to contour the laminate fabrication mold.

Cantilever Frequencies

Table 4 gives the first six natural frequencies of the cantilever plate for the ten different ply orientations. Table 4(a) presents the results using only bending variables, w, α, β with the 16 element model and 3 DOF per node. For Table 4(b), the element model is reduced to 4 elements (Fig. 4(a)). In Table 4(c), results are given for a 4 element model with 5 DOF per node. Comparing corresponding results in Tables 4(a) and (b), it is seen that there is very little difference between the results using the 16 element and the 4 element models for the first and second natural frequencies. The 16 element model usually predicts lower frequencies than the 4 element model for the cases without coupling. For the higher frequencies, there is a larger difference with the 4 element model generally underestimating the natural frequency. Note that the natural frequency of the orthotropic case is the highest for first frequency (first bending) but is low compared to the other cases for the second frequency (first torsion). The fifth and sixth frequencies for cases II to IX are higher than those for case I. For the cases with material coupling (Table 4(c)) all the modes are lower than those without coupling (Table 4(b)). The maximum difference that is obtained for the first frequency (using the case with coupling as a baseline) is 72 percent in case VI, while there is a 91 percent difference in the sixth frequency for case X.

Cantilever Frequencies Comparisons

A comparison of the vibration frequencies of the cantilever plate with and without coupling and with reduced bending stiffness is given in Table 5 for the 16 and 4 element models for case VII. For the 5 DOF per node idealization, the 4 element model first frequency is only 1.5 percent higher than the 16 element model. The largest difference is 13 percent and is in the third frequency. For the 3 DOF per node idealization (no material coupling) both the 16 element and the 4 element models estimate the first frequency to be 44 and 46 percent higher, respectively, compared to the 5 DOF idealization. All the results obtained using the 3 DOF idealization without material coupling overestimate the natural frequencies with a maximum difference of 60 percent for the sixth frequency compared to the 5 DOF idealization. The 3 DOF per node idealization, therefore, is not a realistic representation for a laminate having material coupling. This idealization does not have the stretching (membrane) flexibility that the u and v variables provide the formulation. Therefore, membrane flexibility is necessary to insure accurate frequency results.

The results presented in column 5, Table 5 are for the 3 DOF per node, 4 element model using the reduced stiffness values for the material constants in Table 2. The first and second frequencies are only 3 percent and 7 percent lower, respectively, than those of the 5 DOF per node 16 element model. The sixth frequency differs by less than 6 percent for these two cases. The results indicate more flexibility for the first two frequencies and greater stiffness for the higher ones. Case VII was chosen for these comparisons because it had significant material coupling as shown in Table 1.

Table 6 compares frequency results with and without simulated centrifugal stiffening for the 5 DOF per node idealization, 4 element model. Simulated centrifugal stiffening was introduced by setting the displacement variable u in the x-direction (Fig. 4) equal to zero at the cantilever tip. Note that the first frequency is increased by 20 percent. The remainder are increased by 7 percent or less with the exception of the fifth frequency which is increased by 24 percent. Comparison of these results show that centrifugal stiffening affects the first frequency but has little effect on the next three higher frequencies.

Cantilever Vibration Mode Shapes

A pictorial representation of the first six mode shapes is shown in Figure 3. The mode shapes are normalized with respect to the leading edge tip displacement. Note that for case I, the third mode is a transverse bending mode which does not appear in the isotropic material (aluminum) until mode 6. Also note that the third bending mode of the isotropic material does not appear in the first six modes of case I. Case VII was chosen because it has significant material coupling while case IX has strong bending stiffness and complete coupling characteristics. For case VII, modes 4 and 5 are very close numerically (within 6 percent) as shown in Table 5 for the 5 DOF per node, 16 element idealization. The pictorial representation for these nodes is quite similar. Compared to the isotropic material, there is a slight shift in the nodal line for the second bending mode; the third bending mode appears as the sixth mode for cases VII and IX.

Cantilever Tip Deflection Comparisons

Table 7 compares the tip displacements obtained for case VII using both membrane coupling and reduced stiffness with the displacement obtained without coupling (3 DOF per node idealization). As can be seen, the differences between the coupled and uncoupled cases are from 42 percent at the leading edge to 55 percent at the trailing edge. Using the reduced stiffness values for the material constants, the variation is only 6 to 7 percent. This shows the artificial stiffening that is developed if the idealization is not permitted membrane flexibility. The reduced stiffness is shown to give very good displacement results compared to the 5 DOF model, which is believed to be an adequate representation of the cantilever studied.

The previous discussion leads to the following observation. Use of the reduced stiffness concept to account for bend-stretch coupling in cantilevers made from unsymmetric laminates provides a good approximation for predicting displacement and vibration frequencies. Therefore, finite element computer codes without bend-stretch coupling can be used to analyze nonsymmetric laminates using the reduced stiffness approach. Compared to the case where the bend-stretch coupling is included in the formulation, the reduced stiffness approach has the following advantages: (1) Uses simpler finite element formulation, (2) requires only six stiffness coefficients in the force-deformation relationships, (3) For the same finite element representation of a structure, it will take about one-third the computer storage and will run approximately five times faster.

Summary of Results and Conclusions

The major results and conclusions obtained from this investigation dealing with the structural response of unsymmetric anisotropic, flat, composite cantilevered plates are:

1. Laminate configurations can be selected for the cantilever that will result in the trailing edge tip deflecting either more or less than the leading edge tip where the load is applied.

2. Failure to account for coupling due to nonsymmetry can result in displacement differences that are of a magnitude of the order of the displacement.

3. For the cases investigated, the vibration natural frequencies can be overestimated by as much as 90 percent if coupling due to nonsymmetry is not included.

4. The vibration frequencies of the cantilevers investigated obtained using the 3 DOF per node idealization with reduced bending stiffness are within 3 to 7 percent of those obtained using the 5 DOF per node idealization. The displacements obtained by the same procedure are within 7 percent.

5. Since the deformed shape of an unsymmetric cantilever when subjected to both loads and vibrations exhibits considerable bend-twist coupling, unsymmetric laminate configurations may be selected to yield predetermined deformation under load to provide built-in structural damping to minimize or avoid flutter. The deformed shape can be used to configure the laminate fabrication mold.

6. The reduced stiffness approach using a 5 DOF model as a baseline gives a good approximation for determining displacements and vibration frequencies of unsymmetric anisotropic composite cantilevers.

7. Finite element codes which do not account for bend-stretch coupling can be used to predict displacements and vibration frequencies of unsymmetric laminates via the reduced bending stiffness approach.

Appendix - Derivation of Element Stiffness Matrix

(Refer to Figs. 1 and 3)

The displacement variables per node are u, v, w, α, β. Here u is taken along x, v along y, w along z; α is the rotation in the x-z plane and β in the y-z plane. The interpolation formula.

$$\theta = \sum_{i=1}^{6} N_i \theta_i$$

defines a variable θ within the element in terms of nodal variables θ_i. The vector N is given by

$$N = \begin{Bmatrix} L_1(2L_1 - 1) \\ L_2(2L_2 - 1) \\ L_3(2L_3 - 1) \\ 4L_1L_2 \\ 4L_2L_3 \\ 4L_1L_3 \end{Bmatrix}$$

where the numbers refer to the similarly numbered nodes in Figure 3 and where the area coordinates L_1 for parabolic variation are

$$\begin{Bmatrix} L_1 \\ L_2 \\ L_3 \end{Bmatrix} = \frac{1}{2\Delta} \begin{bmatrix} x_2y_3 - x_3y_2 & y_2 - y_3 & x_3 - x_2 \\ x_2y_1 - x_1y_3 & y_3 - y_1 & x_1 - x_3 \\ x_1y_2 - x_2y_1 & y_1 - y_2 & x_2 - x_1 \end{bmatrix} \begin{Bmatrix} 1 \\ x \\ y \end{Bmatrix}$$

where

$$2\Delta = \text{dET} \begin{bmatrix} 1 & x_1 & y_1 \\ 1 & x_2 & y_2 \\ 1 & x_3 & y_3 \end{bmatrix}$$

Within the element the coordinates can be written

$$x = \sum_{i=1}^{6} N_i x_i$$

$$y = \sum_{i=1}^{6} N_i y_i$$

$$z = \sum_{i=1}^{6} N_i z_i$$

Using the same interpolation functions, the displacement variables are

$$u = \sum_{i=1}^{6} N_i u_i \qquad v = \sum_{i=1}^{6} N_i v_i$$

$$w = \sum_{i=1}^{6} N_i w_i \qquad \alpha = \sum_{i=1}^{6} N_i \alpha_i$$

$$\beta = \sum_{i=1}^{6} N_i \beta_i$$

In terms of the area coordinates the strain-displacement relationships in familiar form are (subscripts denote direction, Fig. 3):

$$\varepsilon_{xx} = e_{xx} - zk_{xx}$$

$$\varepsilon_{yy} = e_{yy} - zk_{yy}$$

$$\varepsilon_{xy} = e_{xy} - zk_{xy} + z^2K_{xy}$$

$$\varepsilon_{xz} = e_{xz}$$

$$\varepsilon_{yz} = e_{yz}$$

where

$$e_{xx} = \frac{\partial u}{\partial x} - \frac{w}{R_1}$$

$$e_{yy} = \frac{\partial v}{\partial y} - \frac{w}{R_2}$$

$$e_{xy} = \frac{\partial u}{\partial y} + \frac{\partial v}{\partial x}$$

$$k_{xx} = \frac{\partial \alpha}{\partial x} - \frac{1}{R_1}\frac{\partial u}{\partial x}$$

$$k_{yy} = \frac{\partial \beta}{\partial y} - \frac{1}{R_2}\frac{\partial v}{\partial y}$$

$$k_{xy} = \frac{\partial \alpha}{\partial y} + \frac{\partial \beta}{\partial x} - \frac{1}{R_1}\frac{\partial u}{\partial y} - \frac{1}{R_2}\frac{\partial v}{\partial x}$$

$$K_{xy} = -\frac{1}{R_1}\frac{\partial \alpha}{\partial y} - \frac{1}{R_2}\frac{\partial \beta}{\partial x}$$

$$e_{xz} = \alpha + \frac{\partial w}{\partial x} + \frac{u}{R_1}$$

$$e_{yz} = \beta + \frac{\partial w}{\partial y} + \frac{v}{R_2}$$

The strain-displacement equations can be written

$$\underset{5\times1}{\begin{Bmatrix}\varepsilon_{xx}\\ \varepsilon_{yy}\\ \varepsilon_{xy}\\ \varepsilon_{xz}\\ \varepsilon_{yz}\end{Bmatrix}} = \underset{5\times30}{[B]} \underset{30\times1}{\begin{bmatrix}u_1\\ v_1\\ w_1\\ \alpha_1\\ \beta_1\\ \cdot\\ \cdot\\ \cdot\\ \cdot\\ \beta_6\end{bmatrix}}$$

The stress-strain equations can be written

$$\underset{5\times1}{\begin{Bmatrix}\sigma_{xx}\\ \sigma_{yy}\\ \sigma_{xy}\\ \sigma_{xz}\\ \sigma_{yz}\end{Bmatrix}} = \underset{5\times5}{[E]} \underset{5\times1}{\begin{bmatrix}\varepsilon_{xx}\\ \varepsilon_{yy}\\ \varepsilon_{xy}\\ \varepsilon_{xz}\\ \varepsilon_{yz}\end{bmatrix}}$$

The element stiffness matrix can be written

$$\underset{30\times30}{[K]} = \int_V B^T E B \, dV$$

For a constant thickness thin plate the element stiffness matrix is

$$\underset{30\times30}{[K]} = \int_A B^T D^* B \, dA$$

where

$$[D^*] = \begin{bmatrix} A & C \\ C & D \end{bmatrix}$$

which are known as the plate constitutive equations.

References

1. Bert, C. W. and Francis, P. H., "Composite Material Mechanics: Structural Mechanics," AIAA Journal, Vol. 12, No. 9, Sept. 1974, pp. 1173-1186.

2. Ashton, J. E. and Whitney, J. M., "Theory of Laminated Plates," Vol. 4, Progress in Materials Science Series, Technomic Publ. Co., Stamford, 1970.

3. Chamis, C. C., "Buckling of Anisotropic Composite Plates," Proceedings of the ASCE, Journal of the Structural Div., Vol. 95, No. ST 10, 1969, pp. 2119-2139.

4. Thornton, E. A. and Clary, R. R., "A Correlation Study of Finite-Element Modeling for Vibrations of Composite Material Panels," Composite Materials: Testing and Design (Third Conference), STP 546, American Society for Testing and Materials, 1974, pp. 111-129.

5. Chamis, C. C., "A Theory for Predicting Fiber Composite Laminate Warpage Resulting from Fabrication," presented at the 30th Annual Reinforced Plastics Composites Conf., Washington, D.C., Feb. 4-7, 1975.

6. Chamis, C. C., "Computer Code for the Analysis of Multilayered Fiber Composites - Users Manual," TN D-7013, Mar. 1971, NASA.

Table 1 Summary of stiffnesses for a 12-ply laminate with various ply orientations

[T75-S/epoxy, FVR = 0.60]

Property	Units	0_{12}	$(\pm 45_3)_S$	$+45_2[(\mp 45)_2]_S$ $+45_2$	$+45_6$ -45_6	$[(0,90)_3]_S$	$0_6 90_6$	$(0,+45)_3$ $(-45,90)_3$	$(0,30)_2 0,45$ $-45,90(-60,90)_2$	$(0,90)_3$ 45_6	$(80,-40)_6$
		Case									
		I	II	III	IV	V	VI	VII	VIII	IX	X
A_{11}	10^3 lb/in.	4528	1251	1251	1251	2315	2315	1783	1872	1783	889
A_{12}	10^3 lb/in.	24	1088	1088	1088	24	24	556	467	556	602
A_{13}	10^3 lb/in.	0	0	369	0	0	0	0	154	553	-618
A_{22}	10^3 lb/in.	101	1251	1251	1251	2315	2315	1783	1872	1783	2585
A_{23}	10^3 lb/in.	0	0	369	0	0	0	0	-154	553	-94
A_{33}	10^3 lb/in.	82	1146	1146	1146	82	82	614	525	614	660
A_{44}	10^3 lb/in.	37	37	37	37	37	37	37	37	37	37
A_{55}	10^3 lb/in.	37	37	37	37	37	37	37	37	37	37
C_{11}	10^3 lb	0	0	0	0	0	-55	-32	-43	-18	3.2
C_{12}	10^3 lb	0	0	0	0	0	0	0	0	13	1.9
C_{13}	10^3 lb	0	0	0	-28	0	0	-11	-10	14	-2.7
C_{22}	10^3 lb	0	0	0	0	0	55	32	43	-8.7	-7.0
C_{23}	10^3 lb	0	0	0	-28	0	0	-11	-10	14	-3.4
C_{33}	10^3 lb	0	0	0	0	0	0	0	0	13	1.9
C_{44}	10^3 lb	0	0	0	0	0	0	0	0	0	0
C_{55}	10^3 lb	0	0	0	0	0	0	0	0	0	0
D_{11}	In.-lb	3774	1042	1042	1042	2390	1929	1597	1679	1716	741
D_{12}	In.-lb	20	906	906	906	20	20	352	270	463	502
D_{13}	In.-lb	0	231	546	0	0	0	0	142	461	-515
D_{22}	In.-lb	85	1042	1042	1042	1468	1929	1597	1679	1255	2154
D_{23}	In.-lb	0	231	546	0	0	0	0	-142	461	-78
D_{33}	In.-lb	68	955	955	955	68	68	401	318	511	550
D_{44}	In.-lb	31	31	31	31	31	31	31	31	31	31
D_{55}	In.-lb	31	31	31	31	31	31	31	31	31	31

Table 2 Summary of reduced bending stiffnesses for a 12-ply laminate with various ply orientations [T75-S/epoxy, FVR = 0.60] (For ply orientation, see Table 1)

Property	Units	Case					
		IV	VI	VII	VIII	IX	X
D_{11}	in.-lb	374	606	733	564	682	728
D_{12}	in.-lb	238	6	-66	-52	206	492
D_{13}	in.-lb	0	0	-159	-43	202	-504
D_{22}	in.-lb	374	606	733	564	592	2114
D_{23}	in.-lb	0	0	159	43	189	-77
D_{33}	in.-lb	300	68	287	231	218	540
D_{44}	in.-lb	31	31	31	31	31	31
D_{55}	in.-lb	31	31	31	31	31	31

Table 3 Tip deflection of a cantilevered unsymmetric fiber composite laminated plate (in.) (For ply orientation, see Table 1)

(a) Without coupling (3 DOF, 16 element model)

Location	Case										
	Aluminum	I	II	III	IV	V	VI	VII	VIII	IX	X
LE	0.0510	0.0291	0.0878	0.1020	0.0838	0.0355	0.0405	0.0325	0.0366	0.0452	0.108
1/4	.0483	.0184	.0869	.0986	.0837	.0262	.0306	.2093	.0319	.0385	.116
1/2	.0453	.0099	.0851	.0950	.0826	.0172	.0212	.0264	.0275	.0326	.124
3/4	.0432	.0038	.0825	.0908	.0807	.0088	.0123	.0240	.0234	.0275	.132
TE	.0408	-.0014	.0788	.0856	.0777	.0007	.0036	.0217	.0194	.0229	.140

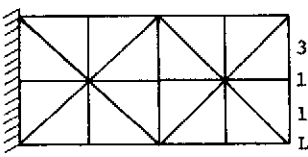

Finite element model

P = 15 lb
a = 2 in.
b = 1 in.
h = 0.1 in.
lb var = 120

(b) With coupling (5 DOF, 16 element model)

Location	Case										
	Aluminum	I	II	III	IV	V	VI	VII	VIII	IX	X
LE	0.0510	0.0291	0.0878	0.1020	0.150	0.0355	0.0887	0.0562	0.0771	0.117	0.108
1/4	.0483	.0184	.0869	.0986	.146	.0262	.0762	.0533	.0724	.101	.117
1/2	.0453	.0099	.0851	.0950	.143	.0172	.0644	.0511	.0685	.087	.124
3/4	.0432	.0038	.0825	.0908	.139	.0088	.0536	.0497	.0656	.075	.133
TE	.0408	-.0014	.0788	.0856	.134	.0007	.0434	.0487	.0631	.063	.141

(c) With reduced stiffness (3 DOF, 16 element model)

Location	Case					
	IV	VI	VII	VIII	IX	X
LE	0.146	0.091	0.060	0.079	0.109	0.109
1/4	.143	.078	.057	.074	.095	.116
1/2	.139	.066	.055	.070	.082	.124
3/4	.136	.055	.053	.067	.071	.132
TE	.131	.045	.052	.065	.061	.140

Table 4 Natural frequencies of a cantilevered unsymmetric fiber composite laminated plate (cycles/sec) (For ply orientation see Table 1)

(a) Without coupling (3 DOF, 16-element model)

Frequency order	Frequency magnitude for case									
	I	II	III	IV	V	VI	VII	VIII	IX	X
1	2 090	824	787	831	1 697	1 535	1 385	1 407	1 327	606
2	2 859	4 747	4 524	4 788	2 650	2 562	4 308	3 947	4 026	3 207
3	8 521	5 522	5 076	5 604	8 810	8 185	7 567	7 682	7 346	5 036
4	10 140	12 304	11 722	12 411	10 145	9 724	13 345	12 476	12 290	8 804
5	11 022	15 862	14 422	16 148	20 355	19 265	18 091	18 390	17 774	14 436
6	15 010	20 715	20 200	20 790	20 960	20 030	23 140	22 370	21 040	16 265

(b) Without coupling (3 DOF, 4-element model)

Frequency order	Frequency magnitude for case									
	I	II	III	IV	V	VI	VII	VIII	IX	X
1	2 092	916	840	936	1 699	1 537	1 398	1 411	1 310	613
2	2 786	4 499	4 025	4 716	2 565	2 470	4 160	3 832	4 069	3 406
3	6 327	5 329	5 096	5 300	8 865	8 259	7 803	7 636	7 136	5 125
4	10 109	11 073	10 186	11 364	11 879	11 320	13 202	13 248	13 034	9 780
5	13 053	15 077	15 203	14 754	16 575	16 203	16 008	15 605	15 626	11 019
6	14 738	18 740	17 084	19 508	19 154	20 398	20 349	20 371	18 265	21 141

(c) With coupling (5 DOF, 4-element model)

Frequency order	Frequency magnitude for case					
	IV	VI	VII	VIII	IX	X
1	647	892	974	867	813	611
2	3 152	2 078	3 445	3 172	2 867	3 390
3	3 803	5 322	6 326	5 551	4 671	5 101
4	7 207	8 007	10 438	9 716	9 601	6 344
5	8 048	8 359	11 285	11 296	9 741	9 727
6	10 811	12 025	14 374	13 311	12 124	10 994

Table 5 Comparison of the vibration frequencies of a cantilevered unsymmetric fiber composite laminated plate (case VII) with and without coupling and with reduced stiffness

Frequency order	Frequency, cycles/sec				
	5 DOF/node with coupling		3 DOF/node without coupling		Bending only with coupling (approx) reduced stiffness 4 element
	16 element	4 element	16 element	4 element	
1	960	974	1 385	1 398	931
2	3 608	3 445	4 308	4 160	3 342
3	5 611	6 326	7 567	7 803	6 128
4	10 685	10 438	13 345	13 202	9 893
5	11 335	11 285	18 091	16 008	13 811
6	14 444	14 374	23 140	20 349	15 285

Table 6 Comparison of the vibration frequencies of a cantilevered unsymmetric fiber composite laminated plate with and without simulated centrifugal stiffening

[Case VII, Table 1, 5 DOF, 16-element model]

Frequency order	Frequency, cycles/sec		Percent difference
	Without stiffening	With stiffening	
1	974	1 160	20
2	3 445	3 570	4
3	6 326	6 793	7
4	10 438	10 540	1
5	11 285	13 950	24
6	14 374	15 440	7

Table 7 Comparison of the tip displacements of a cantilevered unsymmetric fiber composite laminated plate

[Case VII, Table 1, 16-element model]

Location	Displacement, in.		
	Without coupling (3 DOF)	With coupling (5 DOF)	Reduced stiffness (3 DOF)
LE	0.0325	0.0562	0.060
1/4	.0293	.0533	.057
1/2	.0264	.0511	.055
3/4	.0240	.0497	.053
TE	.0217	.0487	.052

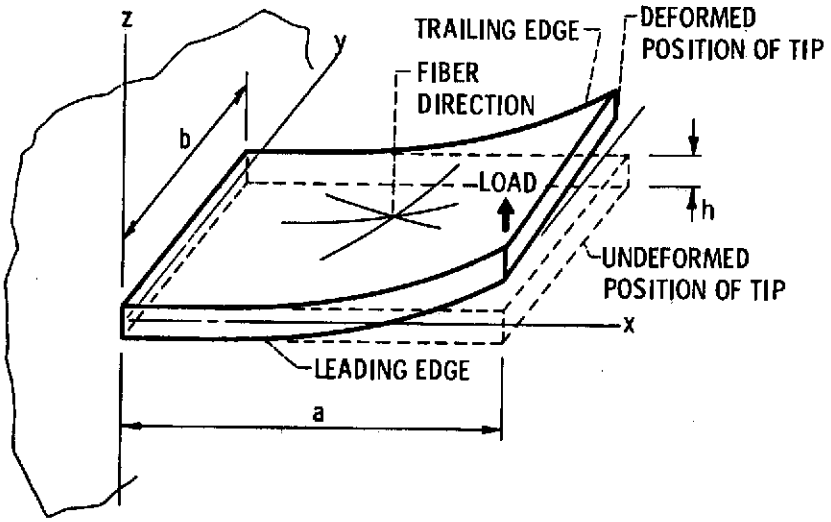

Figure 1. - Schematic of the deformation (bending and twisting) of a cantilevered unsymmetric fiber composite laminated plate.

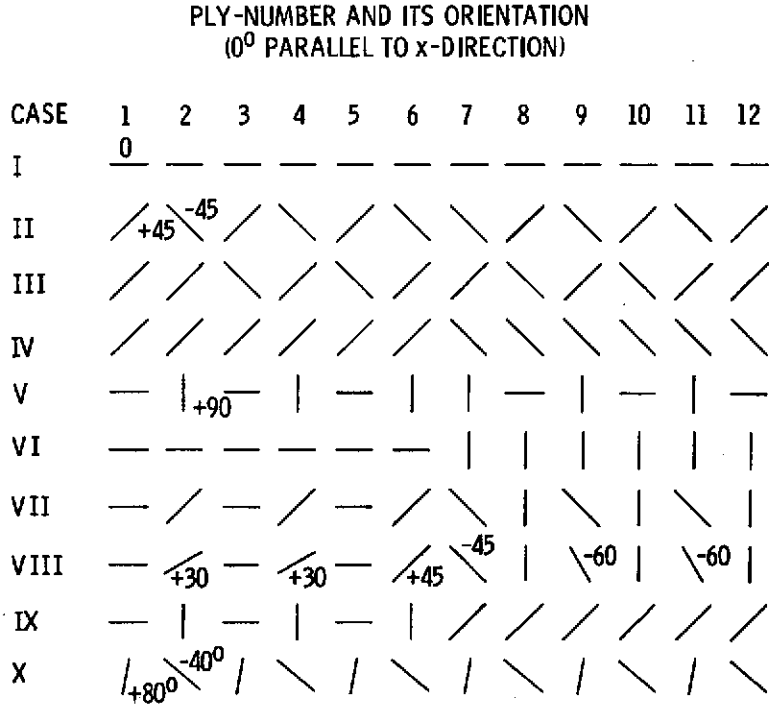

Figure 2. - Ply orientation schematic.

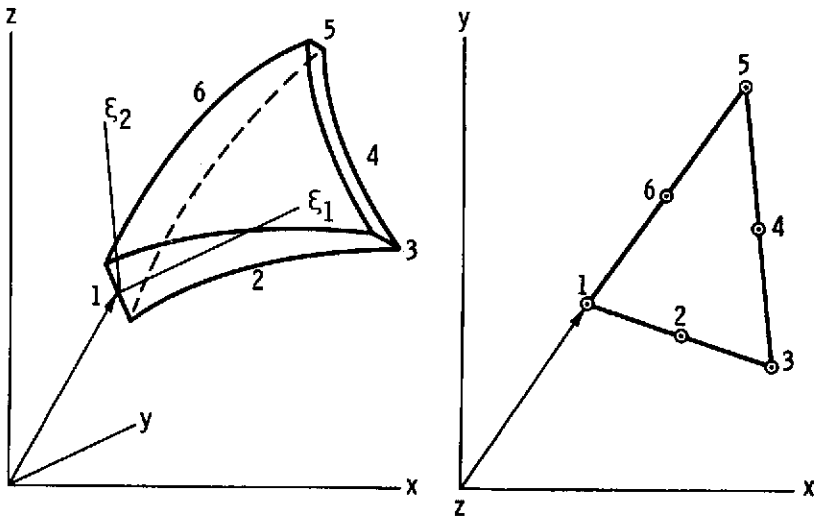

(a) DOUBLY CURVED VARIABLE THICKNESS THIN SHELL.

(b) FLAT THIN PLATE (USED IN PRESENT INVESTIGATION).

Figure 3. - Schematic of the geometry of the 6-node triangular isoparametric finite element.

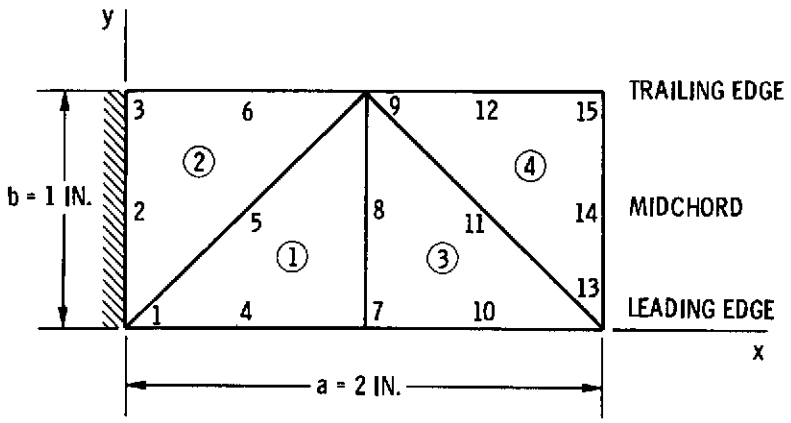

(a) 4-ELEMENT MODEL (15-NODES).

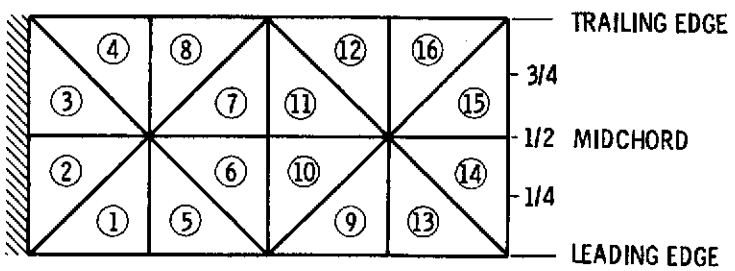

(b) 16-ELEMENT MODEL (45-NODES).

Figure 4. - Finite element representation of cantilever.

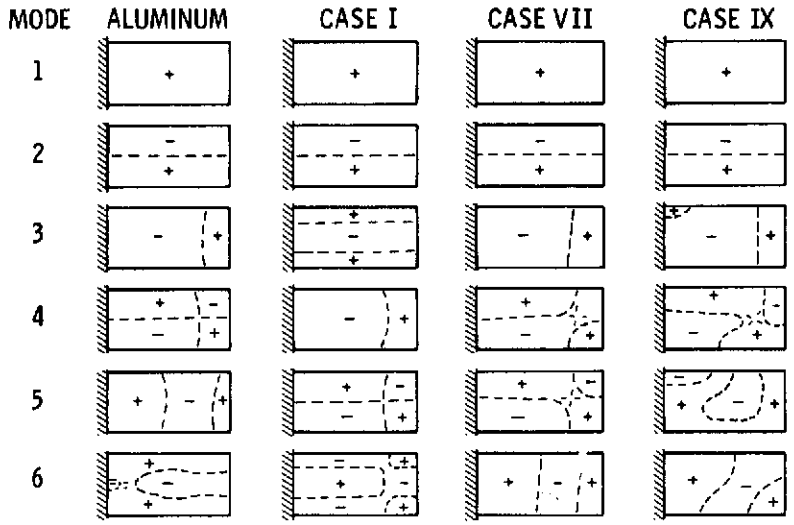

Figure 5. - First six mode shapes of a cantilevered unsymmetric fiber composite laminated plate. (For case identification, see Table I.)